This paper is published as part of a PCCP Themed Issue on:
Physical Chemistry of Aerosols

Guest Editors: Ruth Signorell and Allan Bertram (University of British Columbia)

Editorial

Physical Chemistry of Aerosols
Phys. Chem. Chem. Phys., 2009, **DOI:** 10.1039/b916865f

Perspective

Reactions at surfaces in the atmosphere: integration of experiments and theory as necessary (but not necessarily sufficient) for predicting the physical chemistry of aerosols
Barbara J. Finlayson-Pitts, *Phys. Chem. Chem. Phys.*, 2009, **DOI:** 10.1039/b906540g

Papers

Water uptake of clay and desert dust aerosol particles at sub- and supersaturated water vapor conditions
Hanna Herich, Torsten Tritscher, Aldona Wiacek, Martin Gysel, Ernest Weingartner, Ulrike Lohmann, Urs Baltensperger and Daniel J. Cziczo, *Phys. Chem. Chem. Phys.*, 2009, **DOI:** 10.1039/b901585j

Secondary organic aerosol formation from multiphase oxidation of limonene by ozone: mechanistic constraints *via* two-dimensional heteronuclear NMR spectroscopy
Christina S. Maksymiuk, Chakicherla Gayahtri, Roberto R. Gil and Neil M. Donahue, *Phys. Chem. Chem. Phys.*, 2009, **DOI:** 10.1039/b820005j

DRIFTS studies on the photodegradation of tannic acid as a model for HULIS in atmospheric aerosols
Scott Cowen and Hind A. Al-Abadleh, *Phys. Chem. Chem. Phys.*, 2009, **DOI:** 10.1039/b905236d

Infrared spectroscopy of ozone and hydrogen chloride aerosols
Chris Medcraft, Evan G. Robertson, Chris D. Thompson, Sigurd Bauerecker and Don McNaughton, *Phys. Chem. Chem. Phys.*, 2009, **DOI:** 10.1039/b905424n

IR spectroscopy of physical and chemical transformations in cold hydrogen chloride and ammonia aerosols
Evan G. Robertson, Chris Medcraft, Ljiljana Puskar, Rudolf Tuckermann, Chris D. Thompson, Sigurd Bauerecker and Don McNaughton, *Phys. Chem. Chem. Phys.*, 2009, **DOI:** 10.1039/b905425c

Formation of naproxen–polylactic acid nanoparticles from supercritical solutions and their characterization in the aerosol phase
Moritz Gadermann, Simran Kular, Ali H. Al-Marzouqi and Ruth Signorell, *Phys. Chem. Chem. Phys.*, 2009, **DOI:** 10.1039/b901744e

Measurements and simulations of the near-surface composition of evaporating ethanol–water droplets
Christopher J. Homer, Xingmao Jiang, Timothy L. Ward, C. Jeffrey Brinker and Jonathan P. Reid, *Phys. Chem. Chem. Phys.*, 2009, **DOI:** 10.1039/b904070f

Effects of dicarboxylic acid coating on the optical properties of soot
Huaxin Xue, Alexei F. Khalizov, Lin Wang, Jun Zheng and Renyi Zhang, *Phys. Chem. Chem. Phys.*, 2009, **DOI:** 10.1039/b904129j

Spectroscopic evidence for cyclical aggregation and coalescence of molecular aerosol particles
J. P. Devlin, C. A. Yinnon and V. Buch, *Phys. Chem. Chem. Phys.*, 2009, **DOI:** 10.1039/b905018n

Photoenhanced ozone loss on solid pyrene films
Sarah A. Styler, Marcello Brigante, Barbara D'Anna, Christian George and D. J. Donaldson, *Phys. Chem. Chem. Phys.*, 2009, **DOI:** 10.1039/b904180j

Quantifying the reactive uptake of OH by organic aerosols in a continuous flow stirred tank reactor
Dung L. Che, Jared D. Smith, Stephen R. Leone, Musahid Ahmed and Kevin R. Wilson, *Phys. Chem. Chem. Phys.*, 2009, **DOI:** 10.1039/b904418c

Laboratory study of the interaction of HO_2 radicals with the NaCl, NaBr, $MgCl_2 \cdot 6H_2O$ and sea salt surfaces
Ekaterina Loukhovitskaya, Yuri Bedjanian, Igor Morozov and Georges Le Bras, *Phys. Chem. Chem. Phys.*, 2009, **DOI:** 10.1039/b906300e

Kinetics of the heterogeneous reaction of nitric acid with mineral dust particles: an aerosol flowtube study
A. Vlasenko, T. Huthwelker, H. W. Gäggeler and M. Ammann, *Phys. Chem. Chem. Phys.*, 2009, **DOI:** 10.1039/b904290n

Timescale for hygroscopic conversion of calcite mineral particles through heterogeneous reaction with nitric acid
Ryan C. Sullivan, Meagan J. K. Moore, Markus D. Petters, Sonia M. Kreidenweis, Greg C. Roberts and Kimberly A. Prather, *Phys. Chem. Chem. Phys.*, 2009, **DOI:** 10.1039/b904217b

Mid-infrared complex refractive indices for oleic acid and optical properties of model oleic acid/water aerosols
Shannon M. McGinty, Marta K. Kapala and Richard F. Niedziela, *Phys. Chem. Chem. Phys.*, 2009, **DOI:** 10.1039/b905371a

A study of oleic acid and 2,4-DHB acid aerosols using an IR-VUV-ITMS: insights into the strengths and weaknesses of the technique
Sarah J. Hanna, Pedro Campuzano-Jost, Emily A. Simpson, Itamar Burak, Michael W. Blades, John W. Hepburn and Allan K. Bertram, *Phys. Chem. Chem. Phys.*, 2009, **DOI:** 10.1039/b904748d

Deliquescence behaviour and crystallisation of ternary ammonium sulfate/dicarboxylic acid/water aerosols
L. Treuel, S. Pederzani and R. Zellner, *Phys. Chem. Chem. Phys.*, 2009, **DOI:** 10.1039/b905007h

Laboratory chamber studies on the formation of organosulfates from reactive uptake of monoterpene oxides
Yoshiteru Iinuma, Olaf Böge, Ariane Kahnt and Hartmut Herrmann, *Phys. Chem. Chem. Phys.*, 2009, **DOI:** 10.1039/b904025k

Measurement of fragmentation and functionalization pathways in the heterogeneous oxidation of oxidized organic aerosol
Jesse H. Kroll, Jared D. Smith, Dung L. Che, Sean H. Kessler, Douglas R. Worsnop and Kevin R. Wilson, *Phys. Chem. Chem. Phys.*, 2009, **DOI:** 10.1039/b905289e

Using optical landscapes to control, direct and isolate aerosol particles
Jon B. Wills, Jason R. Butler, John Palmer and Jonathan P. Reid, *Phys. Chem. Chem. Phys.*, 2009, **DOI:** 10.1039/b908270k

Reactivity of oleic acid in organic particles: changes in oxidant uptake and reaction stoichiometry with particle oxidation
Amy M. Sage, Emily A. Weitkamp, Allen L. Robinson and Neil M. Donahue, *Phys. Chem. Chem. Phys.*, 2009, **DOI:** 10.1039/b904285g

Surface tension of mixed inorganic and dicarboxylic acid aqueous solutions at 298.15 K and their importance for cloud activation predictions
Alastair Murray Booth, David Owen Topping, Gordon McFiggans and Carl John Percival, *Phys. Chem. Chem. Phys.*, 2009, **DOI:** 10.1039/b906849j

Kinetics of the heterogeneous conversion of 1,4-hydroxycarbonyls to cyclic hemiacetals and dihydrofurans on organic aerosol particles
Yong Bin Lim and Paul J. Ziemann, *Phys. Chem. Chem. Phys.*, 2009, **DOI:** 10.1039/b904333k

Time-resolved molecular characterization of limonene/ozone aerosol using high-resolution electrospray ionization mass spectrometry
Adam P. Bateman, Sergey A. Nizkorodov, Julia Laskin and Alexander Laskin, *Phys. Chem. Chem. Phys.*, 2009, **DOI:** 10.1039/b905288g

Cloud condensation nuclei and ice nucleation activity of hydrophobic and hydrophilic soot particles
Kirsten A. Koehler, Paul J. DeMott, Sonia M. Kreidenweis, Olga B. Popovicheva, Markus D. Petters, Christian M. Carrico, Elena D. Kireeva, Tatiana D. Khokhlova and Natalia K. Shonija, *Phys. Chem. Chem. Phys.*, 2009, **DOI:** 10.1039/b905334b

Effective broadband refractive index retrieval by a white light optical particle counter
J. Michel Flores, Miri Trainic, Stephan Borrmann and Yinon Rudich, *Phys. Chem. Chem. Phys.*, 2009, **DOI:** 10.1039/b905292e

Influence of gas-to-particle partitioning on the hygroscopic and droplet activation behaviour of α-pinene secondary organic aerosol
Zsófia Jurányi, Martin Gysel, Jonathan Duplissy, Ernest Weingartner, Torsten Tritscher, Josef Dommen, Silvia Henning, Markus Ziese, Alexej Kiselev, Frank Stratmann, Ingrid George and Urs Baltensperger, *Phys. Chem. Chem. Phys.*, 2009, **DOI:** 10.1039/b904162a

Reactive uptake studies of NO_3 and N_2O_5 on alkenoic acid, alkanoate, and polyalcohol substrates to probe nighttime aerosol chemistry
Simone Gross, Richard Iannone, Song Xiao and Allan K. Bertram, *Phys. Chem. Chem. Phys.*, 2009, **DOI:** 10.1039/b904741g

Organic nitrate formation in the radical-initiated oxidation of model aerosol particles in the presence of NO_x
Lindsay H. Renbaum and Geoffrey D. Smith, *Phys. Chem. Chem. Phys.*, 2009, **DOI:** 10.1039/b909239k

Dynamics and mass accommodation of HCl molecules on sulfuric acid–water surfaces
P. Behr, U. Scharfenort, K. Ataya and R. Zellner, *Phys. Chem. Chem. Phys.*, 2009, **DOI:** 10.1039/b904629a

Structural stability of electrosprayed proteins: temperature and hydration effects
Erik G. Marklund, Daniel S. D. Larsson, David van der Spoel, Alexandra Patriksson and Carl Caleman, *Phys. Chem. Chem. Phys.*, 2009, **DOI:** 10.1039/b903846a

Tandem ion mobility-mass spectrometry (IMS-MS) study of ion evaporation from ionic liquid-acetonitrile nanodrops
Christopher J. Hogan Jr and Juan Fernández de la Mora, *Phys. Chem. Chem. Phys.*, 2009, **DOI:** 10.1039/b904022f

Homogeneous ice freezing temperatures and ice nucleation rates of aqueous ammonium sulfate and aqueous levoglucosan particles for relevant atmospheric conditions
Daniel Alexander Knopf and Miguel David Lopez, *Phys. Chem. Chem. Phys.*, 2009, **DOI:** 10.1039/b903750k

Water uptake of clay and desert dust aerosol particles at sub- and supersaturated water vapor conditions

Hanna Herich,[a] Torsten Tritscher,[b] Aldona Wiacek,†[a] Martin Gysel,[b] Ernest Weingartner,[b] Ulrike Lohmann,[a] Urs Baltensperger[b] and Daniel J. Cziczo‡*[a]

Received 23rd January 2009, Accepted 13th March 2009
First published as an Advance Article on the web 1st April 2009
DOI: 10.1039/b901585j

Airborne mineral dust particles serve as cloud condensation nuclei (CCN), thereby influencing the formation and properties of warm clouds. It is therefore of atmospheric interest how dust aerosols with different mineralogy behave when exposed to high relative humidity (RH) or supersaturation (SS) with respect to liquid water. In this study the subsaturated hygroscopic growth and the supersaturated cloud condensation nucleus activity of pure clays and real desert dust aerosols were determined using a hygroscopicity tandem differential mobility analyzer (HTDMA) and a cloud condensation nuclei counter (CCNC), respectively. Five different illite, montmorillonite and kaolinite clay samples as well as three desert dust samples (Saharan dust (SD), Chinese dust (CD) and Arizona test dust (ATD)) were investigated. Aerosols were generated both with a wet and a dry disperser. The water uptake was parameterized *via* the hygroscopicity parameter κ. The hygroscopicity of dry generated dust aerosols was found to be negligible when compared to processed atmospheric aerosols, with CCNC derived κ values between 0.00 and 0.02 (the latter corresponds to a particle consisting of 96.7% by volume insoluble material and $\sim$3.3% ammonium sulfate). Pure clay aerosols were generally found to be less hygroscopic than natural desert dust particles. The illite and montmorillonite samples had $\kappa \sim 0.003$. The kaolinite samples were less hygroscopic and had $\kappa = 0.001$. SD ($\kappa = 0.023$) was found to be the most hygroscopic dry-generated desert dust followed by CD ($\kappa = 0.007$) and ATD ($\kappa = 0.003$). Wet-generated dust showed an increased water uptake when compared to dry-generated samples. This is considered to be an artifact introduced by redistribution of soluble material between the particles. Thus, the generation method is critically important when presenting such data. These results indicate any atmospheric processing of a fresh mineral dust particle which leads to the addition of more than $\sim$3% soluble material will significantly enhance its hygroscopicity and CCN activity.

Introduction

Atmospheric aerosol particles are able to affect chemical, microphysical, and radiative atmospheric processes which makes them important when considering both natural and anthropogenic climate forcing. On the one hand, they absorb and scatter radiation (the 'direct aerosol effect')[1,2] while on the other hand they act as cloud condensation nuclei (CCN) and ice nuclei (IN) leading to cloud formation and growth as well as influencing albedo, persistence, and other cloud properties (the 'indirect aerosol effect').[3–5] Mineral dust particles derived from windblown soils and deserts are one of the most globally abundant natural aerosol species and, according to a 16-model average, they are second in emitted mass only to sea salt and highest in overall atmospheric burden.[6] Depending on their origin, mineral dust particles can contain various constituents such as alumino-silicates, carbonates, and miscellaneous metal oxides.[7] Different dust species can be distinguished by electron microscopy or single particle mass spectrometry.[8] Dust characteristics of atmospheric and climatic interest were summarized in a recent review.[9]

Dust aerosols can undergo a variety of chemical reactions with gaseous precursors in the atmosphere during transport. Their surface can provide a medium for heterogeneous chemical reactions, *e.g.* N_2O_5 hydrolysis,[10] SO_2 oxidation[11] and HO_2 uptake.[12] Several laboratory studies have investigated how pure mineral dusts behave in environments with high relative humidity (RH) in terms of, *e.g.* the uptake of nitric acid.[13,14] It has been shown that both the ambient RH and mineralogy are highly important for reactivity.[9,15]

In terms of microphysical effects dust aerosols have been found to be an important source of IN[16–19] and laboratory studies show that clay minerals in particular (*e.g.*, montmorillonite, kaolinite or illite) have effective ice nucleating properties.[20–22] Different clays were found to nucleate ice with different efficiencies, however. For example montmorillonite was found to be a more efficient IN than

[a] *Institute for Atmospheric and Climate Science, ETH Zurich, CH-8092, Zurich, Switzerland*
[b] *Laboratory of Atmospheric Chemistry, Paul Scherrer Institut, Villigen, CH-5232, Switzerland*
† Now at: Dept of Physics and Atmospheric Science, Dalhousie University, Halifax, Nova Scotia, Canada.
‡ Now at: Pacific Northwest National Laboratory, Richland, WA, United States.

 This journal is © the Owner Societies 2009

kaolinite.[23] The chemical composition of ice nuclei may have significant implications for the indirect aerosol effect, as shown in a modeling study.[24]

From field measurements, mineral dust aerosols are generally found to be non-hygroscopic[25,26] although aged species show somewhat more hydrophilic behavior.[27] Global models that include the mineral dust aerosol component normally assume it to be fully insoluble, *i.e.* non-hygroscopic. The common approach used in numerical models is that dusts are only able to act as CCN after being coated with some fraction of soluble material.[28–32] Nonetheless, as we will show in this paper, unprocessed mineral dust particles are able to act as CCN at 0.2% SS for sizes above 200–400 nm diameter.

The soluble fraction of dust not only influences its role in cloud formation processes but it is also a controlling factor in dust removal by wet deposition. This is especially true for the pathway involving nucleation scavenging in clouds. Water uptake will also affect dust particle size and density, influencing the dry deposition pathway predominantly *via* gravitational settling. A recent study[6] found a high diversity among 16 global models with respect to the emission, deposition, burden, and residence time of six major aerosol components. For sea salt and dust, this comparison found that the models neither agreed on the split between wet and dry deposition, nor on that between sedimentation and other dry deposition processes. Furthermore, there was an extremely high diversity for the uptake of ambient water vapor. While it was noted that the disagreement over deposition pathway was influenced by disagreement in emitted quantities, an improved representation of aerosol water content in global models was identified as a "high priority" necessary for improved estimates of the impact of aerosols on climate. Water content will also modify the optical properties of the suspended particles by changing their size and index of refraction. Uncertainty in radiative effects of the dust particles leads to uncertainty in global model studies of climate and in satellite retrievals of both aerosol and trace gases concentrations. For instance, quantitative satellite retrievals rely on detailed forward models of the underlying radiative transfer, requiring particle physical and optical properties as input parameters.

To understand these effects more information about dust surfaces, specifically the interaction between dust particles and water vapor, is needed. A recent study[33] investigated the water uptake of pure clay minerals spectroscopically and found differences for diverse clays. The greatest water uptake was found for clays that can accommodate swelling and minerals rich in Mg, Fe and Ca. These measurements were performed on bulk samples and, to date, it is neither known to what extent these findings apply to aerosol particles, nor if they apply to desert dusts. Desert dust aerosols have been studied in the laboratory with respect to water uptake but only for a few selected species.[34–37]

Instruments such as a CCNC and a HTDMA are tools that can be used to investigate the water uptake of mineral dust aerosols. With the HTDMA, the water uptake of aerosol particles in terms of the hygroscopic growth factor (GF) can be measured at RH $<$ 100%. With the CCNC the critical supersaturation (S_{crit}) at which aerosols of a certain composition and size activate as CCN can be determined. The aerosol water uptake at sub- and supersaturations is described by the Köhler equation:[38]

$$RH = a_w S_K, \quad (1)$$

where a_w is the water activity and S_K the Kelvin term, accounting for the vapor pressure increase over a curved surface. In this study surface tension of pure water is assumed in the Kelvin term. A simple parameterization of the water activity has been introduced:[39]

$$\kappa = \frac{(GF^3 - 1)(1 - a_w)}{a_w}, \quad (2)$$

which allows, together with eqn (1), a comparison of HTDMA and CCNC measurements.

In this study mineral dust aerosols were generated with either a dry disperser or by atomization from an aqueous solution in order to simulate fresh and processed dust, respectively. Five different clay samples (illite, kaolinites from two sources, montmorillonite and Na-montmorillonite) were analyzed. The results are compared with naturally occurring Saharan dust (SD), China dust (CD) and commercial Arizona test dust (ATD).

Experimental

A schematic illustration of the experimental setup is show in Fig. 1. Aerosols were generated either dry or from an aqueous solution. For wet dust nebulization a custom-built constant output atomizer was used. Dry dust particles were mechanically aerosolized with a custom-built dry dust generator[8] with a cyclone (Model URG-2000-30ED, URG, Chapel Hill, NC, USA) to remove particles exceeding 250 nm diameter. In this case particle free air was added to the aerosol flow to meet the flow rate required for the cyclone. The polydisperse aerosol then passed through a diffusion dryer and a pre-impactor (TSI, Model 1035900, nozzle diameter: 0.071 cm) with a 50% cut point at ~330 nm was used to reduce the incidence of relatively large particles carrying multiple charges. The aerosol flow was split and neutralized with krypton-85 bipolar chargers. A portion of the particles was then size-selected with a differential mobility analyzer (DMA, TSI, Model 3081) and sent to a CCNC (Droplet Measurement Technologies) with a flow rate of 0.5 L min^{-1} and a condensation particle counter

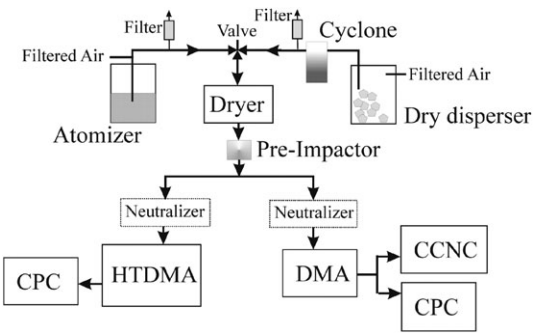

Fig. 1 Schematic of the experimental setup showing wet and dry particle generation in an atomizer and dry disperser, respectively. Hygroscopicity and CCN activity measurements follow in the HTDMA and CCNC, respectively. See text for further details.

(CPC, TSI Model 3772) with a flow rate of 1 L min^{-1}. A detailed description of the CCNC can be found in recent publications.[40,41] With the DMA/CCNC setup, the critical supersaturation required to activate 50% of a monodisperse size-selected aerosol flow was determined. In addition, the DMA and the CPC could be alternately deployed as a scanning mobility particle sizer (SMPS) system to obtain size distributions of the dust samples as described below. The other portion of the aerosol flow was analyzed with a HTDMA, custom-built at the Paul Scherrer Institute and based on a previously described instrument,[42] used in conjunction with another CPC (TSI, Model 3022A) having a flow rate of 0.6 L min^{-1}. The HTDMA had a residence time of 30 s from the entrance of DMA1 to the end of DMA2. HTDMAs determine the water uptake of aerosol particles as a function of RH and dry size. The raw measurement data have been inverted using the algorithm described in a recent study[43] in order to retrieve the hygroscopic growth factor GF, which is defined as $GF(RH) = D_{RH}/D_0$, where D_{RH} is the particle diameter at a certain RH, and D_0 is the dry diameter of the particle ($RH < 10\%$). During this study the HTDMA and the CCNC were periodically calibrated with ammonium sulfate aerosols.

The samples used in this study are listed in Table 1. It should be noted that the composition of dust samples of natural origin may vary from sample to sample. The majority of the samples used here have also been used in previous studies; *e.g.* the illite, kaolinite and montmorillonite were used in a recent sudy[8] as well as the ADT, SD and CD samples.[20]

At the beginning and end of each measurement the number size distribution for each dust sample was obtained using the SMPS. The generation method had a large effect on the size distribution produced. Fig. 2 shows exemplary size distributions of wet and dry generated SD. Dry-generated aerosols had a size mode between 150 and 250 nm diameter where the decrease at larger size can be attributed to removal by the pre-impactor. Wet-generated dust aerosols had a mode at sizes below 50 nm diameter with a rapid decline towards larger sizes. This behavior for wet generated aerosols was more distinct for the collected desert dusts while the size distribution of the pure compounds exhibited a less distinct decrease and often had also a shoulder, or even a bimodal distribution, towards larger sizes. A similar size distribution was also obtained in a study generating ATD with a wet disperser.[35] We believe that the collected desert dusts contain a fraction of soluble material (*e.g.* inorganic salts) which together with the residual contamination of the MilliQ-water, forms this sub-100 nm particle range.

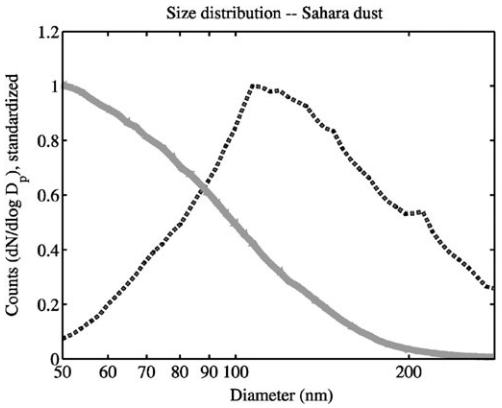

Fig. 2 Number size distribution of wet (grey) and dry (black) generated Saharan dust.

It is assumed that these particles consist of mineral dust but that these aerosols may also have a coating added by the redistribution of soluble material from the larger to the smaller particles. To test this hypothesis composition measurements of dry and wet generated aerosols with an aerosol time-of-flight mass spectrometer (ATOFMS),[44] commercially available from TSI (Model 3800, TSI Inc., MN), were conducted. Several thousand wet and dry aerosol mass spectra of ATD and Na-montmorillonite were acquired with the ATOFMS. A comparison of wet and dry spectra indicate that there are discrepancies in the chemical composition between the two generation methods at the single particle level. Specifically, peaks related to chlorine or nitrates were more pronounced in the spectra of wet-generated aerosols. For this reason we disregard the large number of sub-100 nm aerosol and only data for wet-generated particles with $D = 200$ and 250 nm diameter are presented in these experiments.

Particles of the same size were also used when dry-dispersed for comparison and to minimize potential interferences from multiply charged particles. With the HTDMA the GF was determined at $88 < RH < 94\%$, and, for selected dust samples, humidograms (with $17\% < RH < 94\%$) were obtained. The supersaturation in the CCNC was ramped from 0.07 to 1.0% while keeping the selected dry size constant. The activated fraction as a function of supersaturation, commonly referred to as the S-scan, was fitted with a double sigmoid curve in order to determine the critical supersaturation, S_{crit}, where 50% of the particles act as CCN. Effects of multiple charges were accounted for by taking the 50% cut of the sigmoid representing the singly charged particles.

Table 1 Dust sample properties

Dust samples	Aerosol generation	Product origin
Illite	Dry and wet	Arginotec, NX Nanopowder, B + M Nottenkaemper, Munich, Germany
Kaolinite	Dry and wet	Fluka Ref. 03584 [1318-74-7] Natural origin
Kaolinite (low defect)	Dry (limited sample)	Clay Minerals Society, Chantilly VA, USA, Natural origin
Montmorillonite	Dry and wet	Aldrich, K^{-10}, Cat. 28,152-2 [1318-93-0] Natural origin
Na-montmorillonite	Dry and wet	Clay Minerals Society, Chantilly VA, USA, Natural origin
Arizona test dust	Dry and wet	Powder Technology Inc. (Minnesota, USA)
China desert dust	Dry (limited sample)	Takla Makan Desert, China
Saharan desert dust	Dry and wet	Near Cairo, Egypt

This journal is © the Owner Societies 2009

Results

Aerosol particles of 200 and 250 nm mobility diameter of the eight different dust species listed in Table 1 were analyzed with the HTDMA and CCNC with GF determined in the former and S_{crit} in the latter. The hygroscopicity parameter κ was then determined from each data set. Fig. 3 presents the determined S_{crit} from the CCN data as a function of the aerosol diameter with lines of constant κ shown for clarity. Lines for mixed insoluble/soluble particles with 1% and 5% ammonium sulfate volume fraction (ε_{AS} = 0.01 and ε_{AS} = 0.05) are also shown. In general, all dust particles activated at higher saturations than typical atmospheric aerosol (κ = 0.2 to 0.4 for the lower free troposphere aerosol,[25] $\kappa \approx 0.1$ for secondary organic aerosol,[45] and $\kappa \approx 0.6$ for pure ammonium sulfate aerosol[39]). CCN derived κ values close to zero were found for all samples. These values are in agreement with the general global dust modeling assumption that mineral dusts are non-hygroscopic.[46] Specifically, the determined κ are predominantly found on the order of magnitude below 0.020. A trend in hygroscopicity was apparent, however. The highest S_{crit} and lowest corresponding κ was needed for activation of the dry-generated pure kaolinite clays. The clays illite, montmorillonite and Na-montmorillonite activated at slightly higher saturations than kaolinite but similar to one another and all had κ = 0.002–0.003. For dry generated desert dusts generally lower supersaturations were found. ATD was found to have κ = 0.002–0.003, CD κ = 0.007 and SD κ = 0.023.

Wet-generated dusts in all cases activated at significantly lower supersaturations than the corresponding dry generated aerosols. Again, this bias of the wet generation is an artifact due to soluble material added by a redistribution from the larger to the smaller particles. For this reason samples such as mineral dust should never be brought into solution for aerosol generation if the goal is to mimic fresh emissions. The dry generated dusts, on the other hand, are considered to be representative of fresh windblown emissions.

The mineral dusts showed only minimal growth in the HTDMA even at RH as high as 94%. The observed growth factors are right at the detection limit of the instrument, which was limited during these experiments by the stability of the aerosol source. Uncertainties of the HTDMA derived κ values are therefore generally larger than the observed differences in between the samples. The κ values obtained from the HTDMA data were compared to the CCNC-derived κ values and the results are presented in Fig. 4 with this caveat that the uncertainties associated with the HTDMA data are greater than for the CCN since the instability of the aerosol source did not affect the latter instrument. All except one of the κ values determined from the GFs were found to be below 0.010, which corresponds to ε_{AS} = 0.017. The CD and both kaolinite samples exhibited the lowest GFs. Considering the error range the kaolinite samples indicate a GF $\leq$ 1. GFs $<$ 1 are physically possible due to a restructuring, change in shape, or compaction of an aerosol. A recent study[34] observed a GF $<$ 1 after ATD aerosols was exposed to high RH ($>$95%). Another study[37] found GFs $<$ 1 for ATD aerosols in the RH range from 50%–80% although no restructuring occurred for SD and illite.

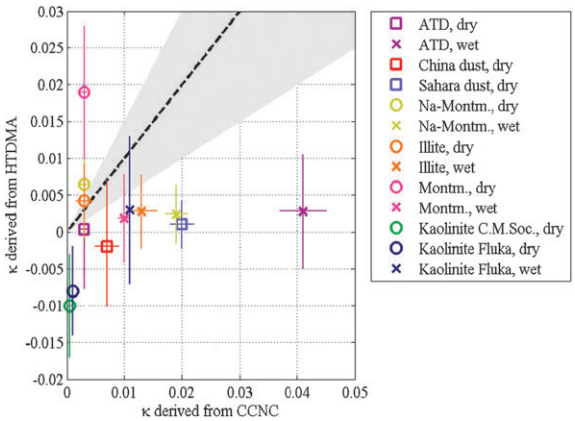

Fig. 4 Averaged κ derived from CCN activity *versus* κ derived from growth factor. Grey area indicates ±50% derivation from 1 : 1 line (black).

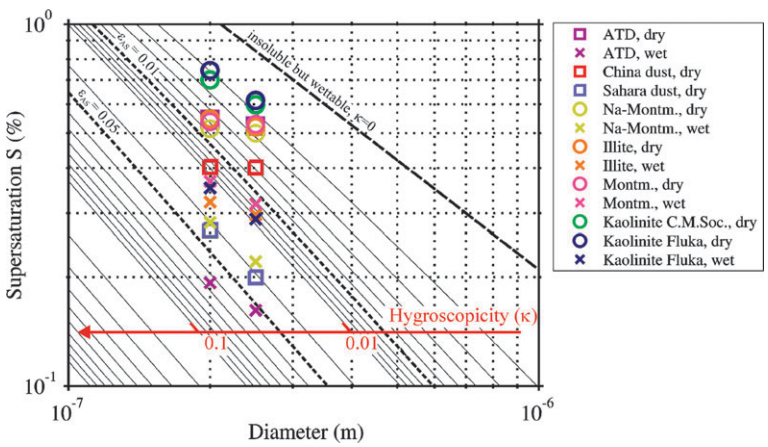

Fig. 3 CCNC-derived critical supersaturations as a function of the particle mobility diameter for dry generated clays (circle), desert dust (square) and wet generated samples (cross). Constant κ lines are shown for reference. Lines to illustrate hypothetical particles with κ = 0.006 and κ = 0.03 corresponding to mixed insoluble/soluble particles with an ammonium sulfate volume fraction of ε_{AS} = 0.01 and ε_{AS} = 0.05, respectively, are also shown.

Within the error limits there is an agreement in the trend of hygroscopicity between the HTDMA and the CCN data with a sole outlying data point for wet generated ATD. The HTDMA derived κ values are, in general, lower than those derived from CCNC data. Due to the detection limit of the HTDMA this trend should not be quantitatively interpreted in terms of the relative hygroscopicity of the different substances. It should be noted that the uncertainty in the HTDMA limits the ability to assess if the higher κ values from the CCNC are due to compounds with limited solubility.

The observation of montmorillonite and illite acting as better CCN than kaolinite is in agreement with a previous study[33] and can be explained by the non-swelling nature of kaolinite. In contrast to this study,[33] which found a higher water uptake for illite than for montmorillonite, we find similar CCN activation for both clay types. In addition, we find the highest water uptake for Na-montmorillonite in comparison to the other montmorillonite and illite types. The order of hygroscopicity may be related to the mineralogy of the dusts; montmorillonite is a hydrate and illite contains substituted $(OH)_2$ and H_2O groups making these species more hygroscopic than kaolinite which has no ion substitutions.

Desert dusts were found to activate at lower supersaturations and had higher GFs than pure clay samples. These findings might be due to desert dusts being internally mixed, *i.e.* they may contain impurities or small amounts of soluble material. Among the desert dusts we find the highest water uptake for SD followed by CD and ATD. The finding of SD being more hygroscopic than ATD has also been observed in a recent study,[37] although in that study larger κ values were determined from HTDMA and CCNC data, with *e.g.* $\kappa \sim 0.050$ for SD and $\kappa \sim 0.030$ for ATD for dry generated samples. This may be partly due to the fact that in that study[37] smaller particle sizes were used. A small trend of increasing κ with decreasing size was also observed in our study.

Conclusions

Mineral dust accounts for a large mass fraction of the tropospheric aerosol loading. This material is not homogeneous, with mineralogy and chemical composition dependent on the source region. Of contemporary interest in atmospheric science is water uptake by mineral dust aerosol as it affects visibility and droplet formation, thereby impacting global climate indirectly.

In this study the CCN activity and hygroscopicity of five different clay and three desert dust aerosol samples were investigated with a CCNC and a HTDMA, respectively. Dust particles were generated by both wet nebulization and dry dispersion. Depending on the dust generation method, different hygroscopicities were found for the same dust species. Specifically, wet nebulization of mineral dust particles results in erroneously high hygroscopicity of particles due to redistribution of soluble material. Hence, nebulized mineral dust aerosols can not be considered representative of fresh wind blow dust emissions.

All investigated dust samples were shown to be wettable ($\kappa \geq 0$) but of limited hygroscopicity/CCN activity ($\kappa \leq 0.02$). The latter value corresponds to an equivalent ammonium sulfate volume fraction of $\varepsilon_{AS} = 0.034$. All investigated species have the potential to activate as CCN at a supersaturation of 0.2% at a diameter of $\gtrsim$200 nm for Saharan dust or $\gtrsim$400 nm diameter for kaolinite. The hygroscopic growth at RHs below saturation was for all samples small, with hygroscopicity parameters below $\kappa = 0.010$. No differentiation between the samples was possible within the sensitivity of the HTDMA in this regime.

The hygroscopicity of two of the desert dusts, ATD[34,35] and SD,[34–36] has been investigated previously. In these studies a similar uptake of water was found. The hygroscopicity of clay samples was examined for bulk material[33] which found a similar relative hygroscopicity, with montmorillonite and illite being more hygroscopic than kaolinite. Although there are clear differences in hygroscopicity between different dusts the CCNC derived hygroscopicity parameters were all in the range $\kappa = 0.020$ to 0.001. These results imply that the water uptake of dust samples, and differences among them, are small when comparing to values for processed atmospheric aerosols which are typically on the order of $1 < \kappa < 0.1$.[47] It should be noted that only a small amount of soluble material may significantly change the hygroscopicity to a larger extent than differences due to mineralogy. Cloud processing or the uptake of gas-phase nitric acid may increase the GF significantly, with the latter having been observed in a study for ATD.[34] It can be assumed that atmospheric processing of fresh mineral dust particles leading to the addition of more than $\sim$3% soluble material will significantly enhance their hygroscopicity and CCN activity.

Acknowledgements

This work was supported by ETH internal research funding, the PNNL Aerosol Initiative and the European Union FP6 infrastructure project EUSAAR (European Supersites for Atmospheric Aerosol Research). We thank Paul DeMott for useful discussions.

References

1 R. A. McCormick and J. H. Ludwig, *Science*, 1967, **156**, 1358.
2 R. J. Charlson and M. J. Pilat, *J. Appl. Meteorol.*, 1969, **8**, 1001.
3 S. Twomey, *J. Atmos. Sci.*, 1977, **34**, 1149.
4 D. Rosenfeld and I. M. Lensky, *Bull. Am. Meteorol.. Soc.*, 1998, **79**, 2457.
5 U. Lohmann and J. Feichter, *Atmos. Chem. Phys.*, 2005, **5**, 715.
6 C. Textor, M. Schulz, S. Guibert, S. Kinne, S. E. Bauer, Y. Balkanski, T. Berntsen, T. Berglen, O. Boucher, M. Chin, F. Dentener, T. Diehl, H. Feichter, D. Fillmore, S. Ghan, P. Ginoux, S. Gong, A. Grini, J. Hendricks, L. Horrowitz, I. Isaksen, T. Iversen, A. Kirkevag, D. Koch, J. E. Kristjansson, M. Krol, A. Lauer, J. F. Lamarque, X. Liu, V. Montanaro, G. Myhre, J. Penner, G. Pitari, S. Reddy, O. Seland, P. Stier, T. Takemura and X. Tie, *Atmos. Chem. Phys.*, 2006, **6**, 1777.
7 T. Claquin, M. Schulz and Y. J. Balkanski, *J. Geophys. Res.*, 1999, **104**(D18), 22243.
8 S. Gallavardin, U. Lohmann and D. J. Cziczo, *Int. J. Mass Spectrom.*, 2008, **274**, 56.
9 C. R. Usher, A. E. Michel and V. H. Grassian, *Chem. Rev.*, 2003, **103**, 4883.
10 F. J. Dentener and P. J. Crutzen, *J. Geophys. Res.*, 1993, **98**, 7149.
11 S. M. Clegg and J. P. D. Abbatt, *Atmos. Chem. Phys.*, 2001, **1**, 73.
12 R. V. Martin, D. J. Jacob, R. M. Yantosca, M. Chin and P. Ginoux, *J. Geophys. Res.*, 2003, **108**(D3), 4097, DOI: 10.1029/2002JD002622.

 This journal is © the Owner Societies 2009

13 C. D. Mashburn, E. K. Frinak and M. A. Tolbert, *J. Geophys. Res.*, 2006, **111**, D15213, , DOI: 10.1029/2005JD006525.
14 A. Vlasenko, S. Sjogren, E. Weingartner, K. Stemmler, H. W. Gaggeler and M. Ammann, *Atmos. Chem. Phys.*, 2006, **6**, 2147.
15 A. Laskin, T. W. Wietsma, B. J. Krueger and V. H. Grassian, *J. Geophys. Res.*, 2005, **110**, D10208, DOI: 10.1029/2004JD005206.
16 K. Sassen, P. J. DeMott, J. M. Prospero and M. R. Poellot, *Geophys. Res. Lett.*, 2003, **30**(12), 1633, DOI: 10.1029/2003GL017371.
17 P. J. DeMott, K. Sassen, M. R. Poellot, D. Baumgardner, D. C. Rogers, S. D. Brooks, A. J. Prenni and S. M. Kreidenweis, *Geophys. Res. Lett.*, 2003a, **30**(14), 1732, DOI: 10.1029/2003GL017410.
18 P. J. DeMott, D. J. Cziczo, A. J. Prenni, D. M. Murphy, S. M. Kreidenweis, D. S. Thomson, R. Borys and D. C. Rogers, *Proc. Natl. Acad. Sci. U. S. A.*, 2003, **100**, 4655.
19 J. Cozic, S. Mertes, B. Verheggen, D. J. Cziczo, S. J. Gallavardin, S. Walter, U. Baltensperger and E. Weingartner, *J. Geophys. Res.*, 2008, **113**, D15209, DOI: 10.1029/2007JD009266.
20 O. Möhler, P. R. Field, P. Connolly, S. Benz, H. Saathoff, M. Schnaiter, R. Wagner, R. Cotton, M. Krämer, A. Mangold and A. J. Heymsfield, *Atmos. Chem. Phys.*, 2006, **6**, 3007.
21 B. Zuberi, A. K. Bertram, C. A. Cassa, L. T. Molina and M. Molina, *Geophys. Res. Lett.*, 2002, **29**, 1504, DOI: 10.1029/2001GL014289.
22 P. Roberts and J. Hallett, *Quart. J. R. Meteorol. Soc.*, 1968, **94**, 25.
23 A. Salam, U. Lohmann, B. Crenna, G. Lesins, P. Klages, D. Rogers, R. Irani, A. MacGillivray and M. Coffin, *Aerosol Sci. Technol.*, 2006, **40**(2), 134.
24 U. Lohmann and K. Diehl, *J. Atmos. Sci.*, 2006, **63**(3), 968.
25 S. Sjogren, M. Gysel, E. Weingartner, M. R. Alfarra, J. Duplissy, J. Cozic, J. Crosier, H. Coe and U. Baltensperger, *Atmos. Chem. Phys.*, 2008, **8**, 5715.
26 H. Herich, L. Kammermann, M. Gysel, E. Weingartner, U. Baltensperger, U. Lohmann and D. J. Cziczo, *J. Geophys. Res.*, 2008, **113**, D16213, DOI: 10.1029/2008JD009954.
27 K. D. Perry, S. S. Cliff and M. P. Jimenez-Cruz, *J. Geophys. Res.*, 2004, **109**, D23S28, DOI: 10.1029/2004JD004979.
28 I. Tegen, S. P. Harrison, K. Kohfeld, I. C. Prentice, M. Coe and M. Heimann, *J. Geophys. Res.*, 2002, **107**(D21), 4576, DOI: 10.1029/2001JD000963.
29 S. L. Gong, L. A. Barrie, J.-P. Blanchet, K. von Salzen, U. Lohmann, G. Lesins, L. Spacek, L. M. Zhang, E. Girard, H. Lin, R. Leaitch, H. Leighton, P. Chylek and P. Huang, *J. Geophys. Res.*, 2003, **108**(D1), 4007.
30 P. Stier, J. Feichter, S. Kinne, S. Kloster, E. Vignati, J. Wilson, L. Ganzeveld, I. Tegen, M. Werner, Y. Balkanski, M. Schulz and O. Boucher, *Atmos. Chem. Phys.*, 2005, **5**, 1125.
31 Y. Yin, S. Wurzler, Z. Levin and T. G. Reisin, *J. Geophys. Res.*, 2002, **107**(D23), 4724, DOI: 10.1029/2001JD001544.
32 S. Wurzler, T. G. Reisin and Z. Levin, *J. Geophys. Res.*, 2000, **105**, 4501.
33 J. D. Schuttlefield, D. Cox and V. H. Grassian, *J. Geophys. Res.*, 2007, **112**, D21303, DOI: 10.1029/2007JD008973.
34 A. Vlasenko, S. Sjogren, E. Weingartner, H. W. Gaggeler and M. Ammann, *Aerosol Sci. Technol.*, 2005, **39**(5), 452.
35 R. J. Gustafsson, A. Orlov, C. L. Badger, P. T. Griffiths, R. A. Cox and R. M. Lambert, *Atmos. Chem. Phys.*, 2005, **5**, 3415.
36 E. R. Gibson, P. K. Hudson and V. H. Grassian, *Geophys. Res. Lett.*, 2006, **33**, L13811, DOI: 10.1029/2006GL026386.
37 K. A. Koehler, S. M. Kreidenweis, P. J. DeMott, M. D. Petters, A. J. Prenni and C. M. Carrico, *Geophys. Res. Lett.*, 2009, in press.
38 H. Köhler, *Trans. Faraday Soc.*, 1936, **32**, 1152.
39 M. D. Petters and S. M. Kreidenweis, *Atmos. Chem. Phys.*, 2007, **7**, 1961.
40 G. C. Roberts and A. Nenes, *Aerosol Sci. Technol.*, 2005, **39**, 206.
41 D. Rose, S. S. Gunthe, E. Mikhailov, G. P. Frank, U. Dusek, M. O. Andreae and U. Pöschl, *Atmos. Chem. Phys.*, 2008, **8**, 1153.
42 J. Duplissy, M. Gysel, S. Sjogren, N. Meyer, N. Good, L. Kammermann, V. Michaud, R. Weigel, S. Martins dos Santos, C. Gruening, P. Villani, P. Laj, K. Sellegri, A. Metzger, G. B. McFiggans, G. Wehrle, R. Richter, J. Dommen, Z. Ristovski, U. Baltensperger and E. Weingartner, *Atmos. Meas. Tech. Discuss.*, 2008, **1**, 127.
43 M. Gysel, G. B. McFiggans and H. Coe, *J. Aerosol Sci.*, 2009, **40**, 134–151.
44 E. Gard, J. E. Mayer, B. D. Morrical, R. Dienes, D. P. Fergenson and K. A. Prather, *Anal. Chem.*, 1997, **69**, 4083–4091.
45 J. Duplissy, M. Gysel, M. R. Alfarra, J. Dommen, A. Metzger, A. S. H. Prevot, E. Weingartner, A. Laaksonen, T. Raatikainen, N. Good, S. F. Turner, G. B. McFiggans and U. Baltensperger, *Geophys. Res. Lett.*, 2008, **35**, L03818, DOI: 10.1029/2007GL031075.
46 I. Tegen, *Quart. Sci. Rev.*, 2003, **22**, 1821.
47 M. O. Andreae and D. Rosenfeld, *Earth Sci. Rev.*, 2008, **89**, 13.